THE JOURNAL OF BIOLOGICAL CHEMISTRY VOL. 287, NO. 12, pp. 9376–9388, March 16, 2012
Published in the U.S.A.

NOX5 in Human Spermatozoa

*EXPRESSION, FUNCTION, AND REGULATION**

Received for publication, October 18, 2011, and in revised form, January 27, 2012 Published, JBC Papers in Press, January 30, 2012, DOI 10.1074/jbc.M111.314955

Boris Musset[‡], Robert A. Clark[§], Thomas E. DeCoursey[‡], Gabor L. Petheo[¶], Miklos Geiszt[¶], Yumin Chen[‖], John E. Cornell[‖], Carlton A. Eddy[**], Robert G. Brzyski[**], and Amina El Jamali[§1]

*From the Departments of [§]Medicine, [‖]Epidemiology and Biostatistics, and **Obstetrics and Gynecology, University of Texas Health Science Center and South Texas Veterans Health Care System, San Antonio, Texas 78229, the [‡]Department of Molecular Biophysics and Physiology, Rush University Medical Center, Chicago, Illinois 60612, and the [¶]Department of Physiology, Faculty of Medicine, Semmelweis University, H-1085 Budapest, Hungary*

Background: The identity of the reactive oxygen species (ROS)-producing enzyme(s) in human spermatozoa remains uncertain.
Results: NOX5 NADPH oxidase, but not NOX1/2/4, is expressed in human spermatozoa and produces superoxide. Inhibition of NOX5 activity reduces spermatozoa motility.
Conclusion: NOX5 is the main source of superoxide and is implicated in human spermatozoa motility.
Significance: NOX5 might control the numerous ROS-dependent (patho)physiological processes in human spermatozoa.

Physiological and pathological processes in spermatozoa involve the production of reactive oxygen species (ROS), but the identity of the ROS-producing enzyme system(s) remains a matter of speculation. We provide the first evidence that NOX5 NADPH oxidase is expressed and functions in human spermatozoa. Immunofluorescence microscopy detected NOX5 protein in both the flagella/neck region and the acrosome. Functionally, spermatozoa exposed to calcium ionophore, phorbol ester, or H_2O_2 exhibited superoxide anion production, which was blocked by addition of superoxide dismutase, a Ca^{2+} chelator, or inhibitors of either flavoprotein oxidases (diphenylene iododonium) or NOX enzymes (GKT136901). Consistent with our previous overexpression studies, we found that H_2O_2-induced superoxide production by primary sperm cells was mediated by the non-receptor tyrosine kinase c-Abl. Moreover, the H_V1 proton channel, which was recently implicated in spermatozoa motility, was required for optimal superoxide production by spermatozoa. Immunoprecipitation experiments suggested an interaction among NOX5, c-Abl, and H_V1. H_2O_2 treatment increased the proportion of motile sperm in a NOX5-dependent manner. Statistical analyses showed a pH-dependent correlation between superoxide production and enhanced sperm motility. Collectively, our findings show that NOX5 is a major source of ROS in human spermatozoa and indicate a role for NOX5-dependent ROS generation in human spermatozoa motility.

MacLeod (1) demonstrated as early as 1943 that spermatozoa were able to generate reactive oxygen species (ROS).[2] ROS production by spermatozoa correlates with lipid peroxidation, DNA oxidation, poor sperm function, and reduced fertility (2, 3). However, recent evidence suggests that redox activity is physiologically important in promoting normal sperm function (4–6). Generation of ROS is required for sperm capacitation, the final maturation steps associated with hyperactive motility and a physiological acrosome reaction (7, 8). Despite evidence for both physiologic and pathologic effects of ROS in spermatozoa, the identity of the ROS-producing enzyme(s) remains uncertain.

Numerous studies showed similarity between the ROS-producing enzyme in spermatozoa and the enzymatic system expressed in phagocytes. In these cells, the major ROS precursor is the superoxide anion, which is generated by the single-electron reduction of molecular oxygen by the NOX2 NADPH oxidase complex. NOX5 is a novel isoform of the NOX family of NADPH oxidases that is activated by the binding of Ca^{2+} to its cytosolic N-terminal EF-hand domains (9, 10). It is suggested that Ca^{2+} binding induces a conformational change leading to the interaction of the N terminus of NOX5 with its C-terminal substrate-binding and flavin-containing domains, thereby inducing ROS production (9, 10). Among the five splice variants identified, *NOX5α*, *NOX5β*, *NOX5γ*, and *NOX5δ* (all long forms of *NOX5* designated collectively as *NOX5L*) differ in the N-terminal sequences of their Ca^{2+}-binding domains, whereas the truncated *NOX5*S (short) variant lacks the Ca^{2+}-binding domains altogether (11). Although the *NOX5* gene is widely conserved evolutionarily, it is curiously absent from rodent genomes (12). NOX5 was found in a prostate carcinoma cell line (13), hairy cell leukemia B-cells (14), endothelial cells (15), smooth muscle cells (16), stomach (17), cardiac fibroblasts (18), and Barrett esophagus epithelia (19).

* This work was supported, in whole or in part, by National Institutes of Health Grants T32 HL04776 (to A. E. J.), UL1 RR025767 (to A. E. J.), Clinical and Translational Science Awards pilot funding (to A. E. J.), KL2 RR025766 (to A. E. J.), K01 DK084297 (to A. E. J.), and Career Development Award R01-GM087507 (to T. E. D.) and an award from the Iacocca Family Foundation (to B. M.). Robert Clark is a scientific co-founder, member of the Scientific Advisory Board, and equity holder in GenKyoTex SA, a Swiss biotechnology start-up company with a primary goal of developing clinically useful inhibitors of the NOX family of NADPH oxidases.

[1] To whom correspondence should be addressed: 7703 Floyd Curl Dr., San Antonio, TX 78229-3900. Tel.: 210-567-1992; Fax: 210-567-4654; E-mail: AkoulouzeBik@uthscsa.edu.

[2] The abbreviations used are: ROS, reactive oxygen species; BAPTA, 1,2-bis(2-aminophenoxy)ethane-*N*,*N*,*N*′,*N*′-tetraacetic acid; DPI, diphenylene iodonium; NOX, NADPH oxidase; NOX5, NADPH oxidase NOX5; SOD, superoxide dismutase; PMA, phorbol 12-myristate 13-acetate; Bes, *N*,*N*-bis(2-hydroxyethyl)amino]ethanesulfonic acid.

NOX5 mRNA was initially detected in human testis in 2001 (9), and a Ca^{2+} ionophore was shown to induce ROS generation in human spermatozoa (20). NOX5 protein was detected by immunoblot analysis in equine sperm (21). Although these observations suggest that spermatozoa might express NOX5, to date there are no reports that demonstrate NOX5 expression at the protein level in human spermatozoa. Herein, we present data documenting both the expression and function of NOX5 in human spermatozoa.

EXPERIMENTAL PROCEDURES

Semen Samples and Sperm Isolation—Human semen samples were obtained from patient donors as a part of their clinical evaluation for fertility and reproductive health status. Portions of the samples not required for clinical analyses were de-identified and made available for the research protocols described herein. Under these conditions, the Institutional Review Board determined that the study is exempt from requirements for protocol approval and informed consent. Semen was collected by masturbation into sterile plastic containers and allowed to liquefy for at least 30 min before being processed. The samples were centrifuged (500 × *g*, 15 min) to separate the seminal plasma from spermatozoa, and the pellet washed twice in phosphate-buffered normal saline (pH 7) with 10 mM glucose (PBS-G). The spermatozoa were then counted in a hemocytometer chamber, resuspended in PBS-G at 10^9/ml, and used for superoxide assays. Sperm samples containing leukocytes detected by microscopic examination were excluded from the study. For selected experiments, motile spermatozoa were collected using the swim-up procedure (22, 23). Briefly, the spermatozoa were sedimented by centrifugation (500 × *g*, 15 min) and the tube was then incubated upright for 60 min at 37 °C. Motile spermatozoa that progressed from the pellet into the supernatant (swim-up fraction) were collected by aspiration and counted.

Immunoblot Analysis—Spermatozoa resuspended in lysis buffer A (20 mM HEPES, pH 7.9, 350 mM NaCl, 0.5 mM EDTA, 0.5 mM EGTA, 1 mM $MgCl_2$, 10% glycerol (v/v), 1% Nonidet P-40 (v/v), 10 mM NaF, 0.1 mM Na_3VO_4 (orthovanadate), 8 mM β-glycerophosphate, phosphatase inhibitor mixture I and II (Sigma), and protease inhibitor mixture (Roche Applied Science) were sonicated 3 times for 5 s each (20 watts). Lysates were cleared by centrifugation (10,000 × *g*, 15 min). Aliquots containing 60–200 μg of protein were separated on 4–20% SDS-polyacrylamide gradient gels and transferred to polyvinylidene difluoride (PVDF) membranes. The filters were incubated with antibodies directed against c-Abl (Sigma, clone Abl-148 catalog number A5844), phosphotyrosine 245 c-Abl (Cell Signaling, Danvers, MA; catalog number 2861), NOX5 (kindly provided by William Nauseef, University of Iowa) (24), NOX2 (kindly provided by Mark Quinn, Montana State University), NOX4 (Santa Cruz Biotechnology, Santa Cruz, CA, catalog number sc-301141) or NOX1 (GeneTex, Irvine, CA, catalog number GTX-103888), $p22^{phox}$ (Santa Cruz Biotechnology, catalog number sc-20781), and c-Myc (Santa Cruz Biotechnology, catalog number sc-40). Immunoblotting with H_V1 antibody was performed using an affinity-purified polyclonal antibody that recognizes the intracellular N-terminal domain of the human H_V1 protein (25). Immunoblots using actin antibody (Sigma, catalog number A2066) were used to control for loading. The antigen-antibody complexes were visualized by enhanced chemiluminescence (ECL, Amersham Biosciences, Pittsburgh, PA).

Immunoprecipitation—Total protein extracts of K562, K562/NOX5, or human sperm cells prepared in buffer A (250 μg of protein) were pre-cleared with rabbit IgG (Sigma) and protein A/G-agarose (Santa Cruz Biotechnology), incubated overnight with anti-NOX5, anti-H_V1, or nonspecific IgG antibody as a negative control, and precipitated with protein A/G-agarose for an additional 3 h. The immune complexes were washed with lysis buffer, separated on 4–20% SDS-polyacrylamide gradient gels, and transferred to PVDF membranes. The filters were incubated with anti-NOX5, anti-H_V1, or anti-phosphotyrosine 245 c-Abl antibodies. The antigen-antibody complexes were visualized by enhanced chemiluminescence (ECL, Amersham Biosciences).

Immunostaining—For immunohistological analyses, a drop of spermatozoa suspended in PBS-G was placed on a poly-L-lysine-coated glass slide, fixed in 4% (w/v) paraformaldehyde, and permeabilized with 0.1% Triton X-100 (v/v) for 15 min at 4 °C. Spermatozoa were then subjected to immunostaining using the antibodies described above against NOX5, c-Abl, and phospho-Tyr^{245}-c-Abl along with Cy™ 3- or FITC-conjugated secondary antibody (Zymed Laboratories Inc., San Francisco, CA). Protein expression was visualized on a fluorescence microscope (Zeiss). For negative controls, cells were incubated with isotype-matched control antibodies with no known specificity.

Superoxide Assay—Superoxide generation was measured using a luminol-based chemiluminescence assay (Diogenes reagent, National Diagnostics, Atlanta, GA). We have previously demonstrated the specificity of this assay for superoxide *versus* H_2O_2 (24). Spermatozoa were suspended at 10^9/ml in PBS-G. A 100-μl aliquot of the Diogenes reagent was mixed with 2×10^7 spermatozoa and incubated at 37 °C for 2–4 min. Superoxide generation was measured at baseline and after stimulation with ionomycin (1 μM), phorbol myristate acetate (PMA, 1 μg/ml), or H_2O_2 (100 μM and other concentrations as indicated). Chemiluminescence was measured every 30–60 s for up to 10–15 min using a Clarity™ BioTek luminometer and an integration time of 5 s.

Pharmacologic Inhibitors—Spermatozoa were preincubated for 5 min prior to the superoxide assay with 400 units/ml of superoxide dismutase (SOD), 10 μM diphenylene iodonium (DPI), or 100 μM BAPTA. A preincubation time of 1 h was used for the tyrosine kinase inhibitor imatinib mesylate (50 μM, Novartis Pharma AG, Basel, Switzerland). In some experiments, cells were pre-exposed to the NOX inhibitor 2-(2-chlorophenyl)-4-methyl-5-(pyridin-2-ylmethyl)-1*H*-pyrazolo[4,3-*c*]pyridine-3,6(2H,5H)-dione (GKT136901, 0.5 μM and other concentrations as indicated) for 10 min before exposure to either H_2O_2 or PMA. This compound, kindly provided by GenKyoTex SA (Geneva, Switzerland), is a drug-like small molecule with high affinity and specificity for NOX1 and NOX4 (26, 27) and to a lesser extent for NOX5.

Live Cell Imaging—Spermatozoa suspended in PBS-G were plated on poly-L-lysine-coated glass coverslips (2×10^5 cells/

ml) in PBS-G and loaded with 6 μM fluo-4AM and 300 nM dihydroethidine (Molecular Probes, Carlsbad, CA) 10 min before imaging. Ca^{2+} influx and superoxide production were recorded using a confocal microscope (LSM 510; Carl Zeiss MicroImaging, Inc.) with a ×63/1.4 NA plan-apochromat objective. Fluo-4 and dihydroethidine fluorescence emissions were excited with dual laser at 488/543 nm attenuated to avoid photobleaching and saturation. Detection was through a 545-nm long-pass dichroic mirror and a band-pass filter at 500–530 for fluo-4 and LP560 for dihydroethidine.

Cell Culture and Down-regulation of H_V1 Protein by siRNA—Human leukemia cells stably transfected with an empty vector (K562 cells) or a vector encoding for NOX5 (K562/NOX5) were grown in RPMI medium supplemented with 10% (v/v) fetal bovine serum, plus 100 units/ml of penicillin, and 100 μg/ml of streptomycin and the appropriate selection antibiotic. Cells in the logarithmic phase of growth were transfected with a mixture of H_V1 siRNA (Sigma) or with scrambled siRNA (Sigma) using the Neon system (Invitrogen) according to the manufacturer's recommendations. Cells were tested 48 h after transfection for superoxide production and down-regulation of H_V1 protein was detected by immunoblot using the affinity-purified rabbit polyclonal H_V1 antibody raised against an N-terminal domain of H_V1 human protein (25).

Patch Clamp Analysis—Micropipettes were pulled in several stages using a Flaming-Brown automatic pipette puller (Sutter Instruments, San Rafael, CA) from 7052 glass (Garner Glass Co., Claremont, CA), coated with Sylgard 184 (Dow Corning Corp., Midland, MI), heat polished to a tip resistance between 2 and 10 megaohms. Electrical contact with the pipette solution was achieved by a chloride silver wire. The reference electrode was made from a Ag-AgCl wire connected to the bath through an agar bridge made with Ringer solution (160 mM NaCl, 4.5 mM KCl, 2 mM $CaCl_2$, 1 mM $MgCl_2$, 5 mM HEPES adjusted to pH 7.4). Current signal from the Axopatch 200B (Axon Instruments, Foster City, CA) was recorded on a PC through a Lab View SCB-68 (National Instruments, Austin, TX). Further data analysis was made with Origin 7.5. Seals were formed in Ringer solution in the bath, and the potential was zeroed when the pipette was in contact with the cell. Most measurements were done between 21 and 25 °C.

K562 cells were transferred on chips or pipette into the recording chamber. To leave internal signaling pathways undisturbed, the perforated patch configuration was used. Low access resistance was usually reached after 5–10 min. The perforated patch recording bath and pipette solution contained 50 mM NH_4^+ in the form of $(NH_4)_2SO_4$, 2 mM $MgCl_2$, 5 mM Bes or Pipes buffer, and 1 mM EGTA adjusted to pH 7.0 with tetramethylammonium hydroxide. Solubilized amphotericin B (500 μg/ml; ~45% purity, Sigma) was added to the pipette solution, after first dipping the tip into amphotericin-free solution. To investigate the proton channels "enhanced gating mode," 60 nM PMA was used to stimulate the cells. The protein kinase C (PKC) inhibitor GF109203X (GFX; 3 μM) was used to revert the enhanced gating mode. Holding potential for current families measurements was −60 mV. The holding potential for test pulses applied during application of either PMA or GFX was −30 mV.

Statistical Analysis—Natural log transformations were performed for clinical measures of sperm production and fertility (*e.g.* total number of motile spermatozoa, days of abstinence) and superoxide production prior to analysis. Sperm progression and pH were recoded into three-level categorical variables ≤2, 3, >3, and <8, 8–8.5, >8.5, respectively. The Kruskal-Wallis test was used to evaluate the relationship between pH (<8, 8–8.5, and >8.5) and continuous measures of sperm characteristics including superoxide production, whereas Fisher exact tests were used when the comparison was made with categorical measures of sperm characteristics. Correlations between continuous sperm characteristics and superoxide production were assessed using Spearman rank order correlations. Regression analyses were performed with sperm characteristics as the response variable and each of the ROS measures as explanatory variables. The regression models were run controlling for pH and log abstinence. All statistical tests were two-sided with a significance level of 5%. SAS software version 9.2 (SAS Institute, Cary, NC) was used throughout.

A Dunnett multiple comparison test was used for many of the *in vitro* experiments to adjust for multiple testing when comparing several means against the mean for a common control sample. A two-sided value of $p < 0.05$ was accepted as significant.

RESULTS

NOX5 Expression in Human Spermatozoa—A lysate of pooled spermatozoa from several donors was used for immunoblot analysis with antibody specific for NOX5 or NOX2. The NOX5 antibody detected two main immunoreactive species with apparent molecular masses of ~80 and ~65 kDa (Fig. 1*A*), whereas no bands were observed using NOX2 antibody (Fig. 1*A*). Conversely, human neutrophil (PMN) lysates analyzed in parallel exhibited the presence of NOX2 but not NOX5. In addition, immunoblot analysis of sperm lysates using NOX1 or NOX4 antibody resulted in no detectable signals, whereas appropriate immunoreactive bands were detected in lysates of $CaCo_2$ and kidney cells (Fig. 1*A*), which are known to express NOX1 and NOX4, respectively. These results suggest that the predominant NOX enzyme expressed in human spermatozoa is NOX5.

Because the NOX5 antibody was generated against a GST peptide corresponding to the N terminus of NOX5, including the EF-hand domains present in the long splice variants, such as NOX5β, it was possible that the antibody detected more than one long NOX5 variant. However, because the sequence of the peptide immunogen extended 10 amino acids into the predicted N-terminal domain of the short NOX5 variant, the more rapidly migrating band could have represented NOX5S. To test this possibility we performed immunoblot analysis using anti-NOX5 and anti-Myc on lysates of K562 cells stably overexpressing either NOX5β (24) or Myc-tagged NOX5S (construct kindly provided by Guangjie Cheng, University of Alabama at Birmingham). The data show that the NOX5 antibody recognized only NOX5β, whereas anti-Myc detected only Myc-NOX5S (Fig. 1*B*). Moreover, Myc-NOX5S exhibited an apparent molecular mass of ~55 kDa, which is substantially smaller than either of the bands detected in spermatozoa. We conclude

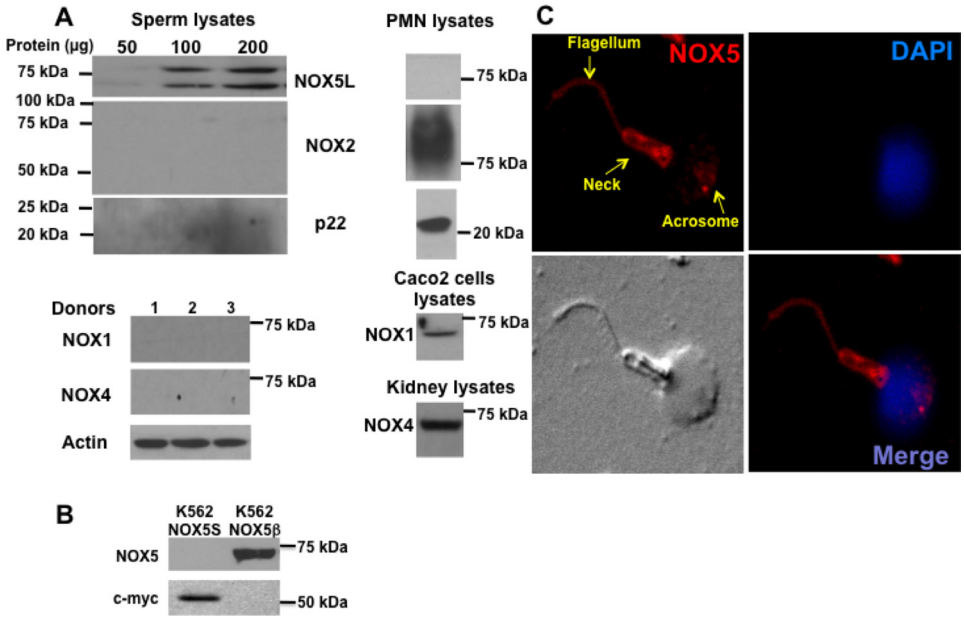

FIGURE 1. **NOX5 expression in human spermatozoa.** *A*, lysates from pooled human spermatozoa from several donors were analyzed by immunoblotting using antibody to NOX2, p22, and NOX5 (*upper panels*) or NOX1 and NOX4 (*lower panels*). Comparisons were made using lysates from human neutrophils (*PMN*), CaCo2 cells, and mouse kidney as positive controls for NOX2, p22, NOX1, and NOX4, respectively. *B*, protein extracts of K562 cells stably transfected with a vector expressing either NOX5β or Myc-tagged NOX5S were analyzed by immunoblot with antibody to either NOX5 or c-Myc. *C*, immunostaining of human spermatozoa with NOX5 antibody and Cy™ 3-conjugated secondary antibody (*top left* and *bottom right*), nuclear staining with DAPI (*top right* and *bottom right*), and differential interference contrast image (*bottom left*).

that the species recognized by anti-NOX5 in sperm lysates represent EF-hand-containing *NOX*5L splice variants. However, because their apparent molecular sizes do not match precisely to the NOX5β expressed in K562 cells, the exact sequences remain to be determined to identify the predominant NOX5L variants present in human spermatozoa.

Immunostaining experiments confirmed the presence of NOX5 in human spermatozoa and showed its localization in the sperm flagellum, neck, and acrosome regions (Fig. 1*C*). These immunoblotting and immunostaining results together demonstrate for the first time that *NOX*5 is expressed in human spermatozoa.

Ca^{2+}-dependent Superoxide Production by Human Spermatozoa—Because the binding of Ca^{2+} to N-terminal EF-hand domains activates NOX5L forms, we assessed whether NOX5 was functional in human sperm by testing the ability of intact spermatozoa to produce superoxide upon exposure to the Ca^{2+} ionophore ionomycin (Fig. 2*A*). Using the superoxide-specific luminol-based Diogenes® reagent chemiluminescence assay (24), we found that ionomycin induced vigorous superoxide production by human spermatozoa. The chemiluminescence signal detected was blocked by addition of SOD, the flavoprotein oxidase inhibitor diphenylene iodonium (DPI), or the Ca^{2+} chelator BAPTA (Fig. 2*A*), indicating that under these conditions we were detecting generation of superoxide anion by a Ca^{2+}-dependent flavoprotein oxidase, such as NOX5. Similar patterns of superoxide generation and blocking agent effects were observed when spermatozoa were exposed to PMA (Fig. 2*B*), a potent phorbol ester activator of PKC that is known to regulate NOX5 activity (28).

We also tested the effect of a newly described NOX inhibitor, GKT136901, to further investigate whether NOX5 accounts for Ca^{2+}-dependent superoxide production. This compound is a potent inhibitor of both NOX1 and NOX4 (K_i = 160 ± 10 and 165 ± 5 nM, respectively) with a ~9-fold selectivity over NOX2 (K_i = 1530 ± 90 nM) (26, 27). Importantly, when tested under the same conditions as described by Laleu *et al.* (26) GKT136901 showed an inhibitory constant of 450 ± 10 nM for NOX5.[3] Our results show that in sperm cells, GKT136901 inhibited the stimulation of superoxide production by PMA in a concentration-dependent manner. GKT136901 was ~10-fold more potent in inhibiting superoxide production stimulated by PMA in sperm cells as compared with neutrophils (Fig. 2*C*). Because human spermatozoa do not express detectable levels of NOX1 or NOX4, these results strongly suggest that the NOX5 protein expressed in human spermatozoa is the functionally active, superoxide-generating enzyme.

Effect of H_2O_2 on Superoxide Production by Human Spermatozoa—We have previously demonstrated that exogenous H_2O_2 induces NOX5 activity in an overexpression system (24). Testing this regulation in human primary cells, we found that H_2O_2 induced a marked burst in superoxide production by human spermatozoa, beginning within 1–2 min after peroxide addition and achieving maximal activity levels, varying somewhat among donors, in 5–10 min (Fig. 3*A*). The induction of superoxide generation was dose-dependent from 1 to 500 μM H_2O_2 (Fig. 3*B*). Subsequent experiments were performed using a standard concentration of 100 μM H_2O_2. As for superoxide generation induced by ionomycin or PMA, the chemiluminescence signal generated by exposure to H_2O_2 was nearly completely abrogated by the addition of SOD, BAPTA, DPI, or

[3] GenKyoTex, personal communication.

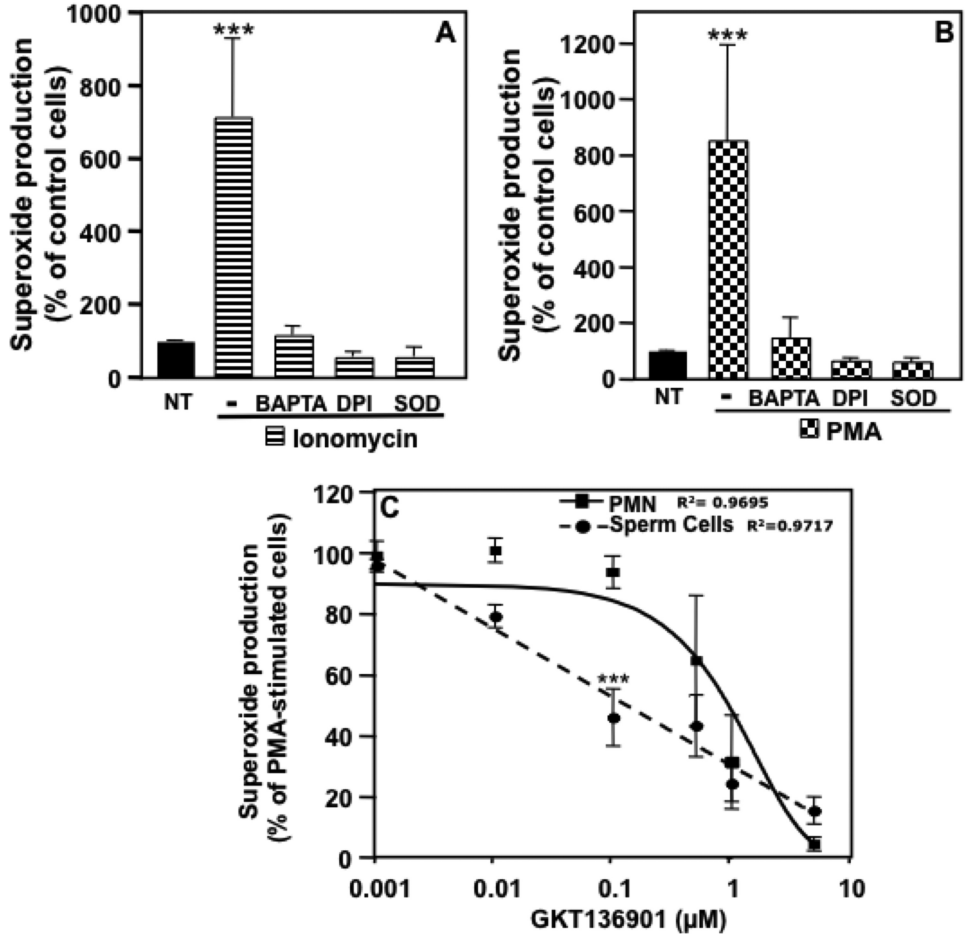

FIGURE 2. **Spermatozoa produce superoxide in a Ca^{2+}-dependent manner.** Human spermatozoa were assayed for superoxide production using the luminol-based Diogenes reagent. Superoxide production was measured using whole sperm cells preincubated or not with various pharmacological agents (BAPTA (100 μM), DPI (10 μM), or SOD (400 units/ml)) and stimulated for 10 min with 1 μM ionomycin (*A*) or 1 μg/ml of PMA (*B*). After normalization by subtraction of the zero time value of the chemiluminescence output, the area *under the curve* was calculated as a measure of total superoxide production and was expressed as a percent of non-treated cells (*NT*). The data expressed are the mean ± S.E. of 4–6 independent experiments. *Asterisks* indicate statistical significance *versus* control cells (NT). ***, $p < 0.001$. *C*, dose-dependent effect of the NOX inhibitor GKT136901 on PMA-stimulated superoxide production by human neutrophils or spermatozoa. The data expressed are the mean ± S.E. of 3–4 independent experiments. *Asterisks* indicate statistical significance *versus* neutrophil cells. ***, $p < 0.001$.

GKT136901 (Fig. 3*C*). Because we have shown that superoxide production by phagocyte NOX2 is also regulated by H_2O_2, we ensured that leukocytes did not account for the superoxide signal stimulated by H_2O_2 in sperm samples by discarding all semen samples in which leukocytes were evident by microscopic observation.

To confirm that spermatozoa produce superoxide when stimulated by H_2O_2, confocal images of spermatozoa freshly loaded with the red fluorescent superoxide probe dihydroethidine were recorded. In addition, we also loaded sperm cells with the Ca^{2+} indicator dye fluo4-AM to detect cytosolic Ca^{2+} responses in parallel with superoxide production. Spermatozoa exposed to H_2O_2 exhibited increases in cytosolic Ca^{2+} levels (*green fluorescence*), as well as the number and intensity of red fluorescing cells, reflecting superoxide generation (Fig. 3*D*). Together with the chemiluminescence data (Fig. 3, *A–C*), these confocal imaging results strongly suggest that superoxide production induced by H_2O_2 was due to Ca^{2+}-mediated activation of the NOX5L proteins expressed in human spermatozoa. The partial co-localization of Ca^{2+} influx and superoxide production suggests partial temporal overlap of these events, as we previously found in NOX5 overexpression studies (24).

Role of c-Abl in H_2O_2-induced Sperm Superoxide Production—We showed previously that c-Abl tyrosine kinase plays a central role in the induction of NOX5 activity in response to H_2O_2 (24). To investigate the potential role of c-Abl in primary human spermatozoa, we assessed its expression and regulation by H_2O_2. Immunoblot analysis showed that c-Abl was expressed in spermatozoa (Fig. 4*A*). Immunostaining demonstrated the presence of c-Abl in the flagellum, neck, and acrosome regions, as well as co-localization with NOX5, as assessed by double immunostaining (Fig. 4*B*). Stimulation of spermatozoa by H_2O_2 induced the phosphorylation of c-Abl on tyrosine 245, an indication of its activation (Fig. 4*C*), as demonstrated by both immunoblot and immunostaining. Pretreatment of human spermatozoa with the selective c-Abl inhibitor imatinib mesylate significantly decreased superoxide production induced by H_2O_2 (Fig. 4*D*). These results suggest that H_2O_2-NOX5 regulation in human spermatozoa is mediated through a c-Abl-dependent signaling pathway.

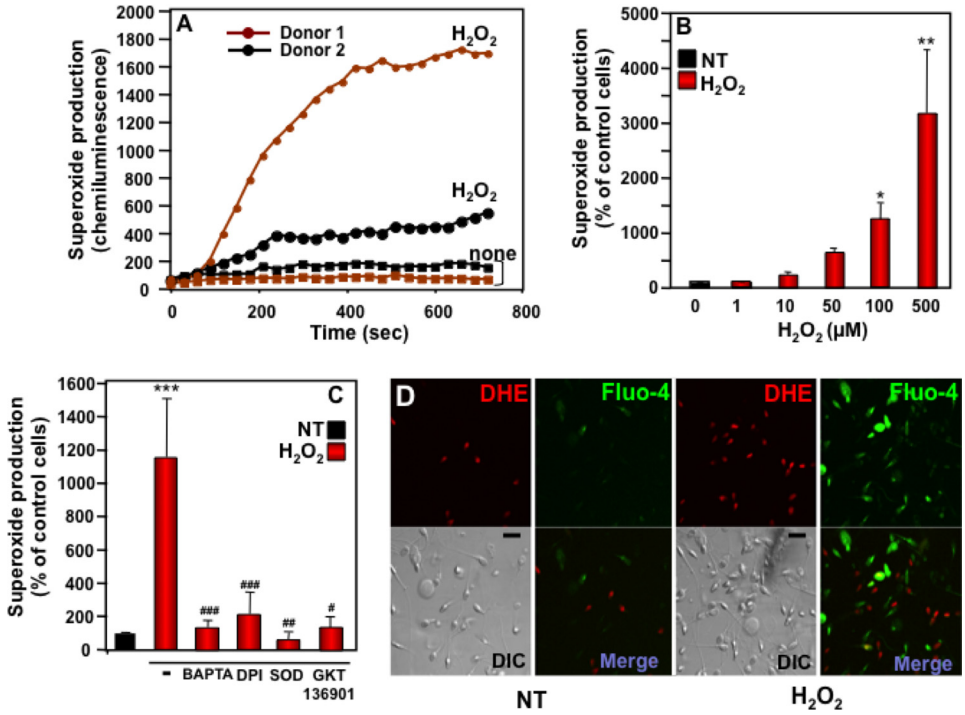

FIGURE 3. **Dose- and time-dependent effects of H_2O_2 on superoxide generation by human spermatozoa.** *A*, superoxide produced by spermatozoa from two different donors with or without 100 μM H_2O_2 was measured over the indicated time course. These results are representative of the range of superoxide responses observed among a total of 94 sperm donors. *B*, superoxide production was measured in sperm cells stimulated for 10 min with various concentrations of H_2O_2 (0–500 μM). *C*, superoxide production stimulated with 100 μM H_2O_2 was determined in sperm cells preincubated with BAPTA (100 μM), DPI (10 μM), SOD (400 units/ml), or GKT136901 (0.5 μM). Superoxide production was determined as described in the legend to Fig. 2 and expressed as a percent of non-treated cells (*NT*). The data expressed in *panels B* and *C* are the mean ± S.E. of 6–10 independent experiments. *Asterisks* indicate statistical significance *versus* control cells without H_2O_2. *, $p < 0.05$; **, $p < 0.01$; ***, $p < 0.001$, and *number signs* indicate statistical significance *versus* cells stimulated with H_2O_2. #, $p < 0.05$; ##, $p < 0.01$; ###, $p < 0.001$. *D*, confocal images of spermatozoa incubated for 10 min without (*NT*) or with H_2O_2 were recorded using a Zeiss microscope. Each set of four photomicrograph *panels* corresponds to superoxide production (red fluorescence, *top left*), Ca^{2+} influx (green fluorescence, *top right*), the differential interference contrast (*DIC*) image (*bottom left*), and a merge picture of the two fluorescent images (*bottom right*). The *scale bar* indicates a size of 10 μm. *DHE*, dihydroethidine.

Superoxide Production by NOX5 Requires H_V1 Proton Channel—It has been recently reported that H_V1 voltage-regulated proton channels present in human spermatozoa are implicated in their motility (29). Because H_V1-dependent proton efflux has been shown to compensate membrane depolarization and intracellular acidification arising from phagocyte NOX2 enzymatic activity (30–33), we hypothesized that the activity of this channel is associated with NOX5-dependent superoxide production in human spermatozoa.

We investigated the potential interaction of NOX5 and H_V1 using K562 cells overexpressing NOX5β. We evaluated the impact of H_V1 function on NOX5 activity using Zn^{2+}, a potent inhibitor of H_V1 proton currents (34), or siRNA to down-regulate the expression of H_V1. We observed that induction of superoxide production in K562/NOX5 cells stimulated by ionomycin, PMA, or H_2O_2 was decreased by 1 mM $ZnCl_2$ (Fig. 5*A*) or H_V1 siRNA (Fig. 5*B*), by 50–70 or 30–50%, respectively. Furthermore, immunoprecipitation experiments showed the presence of NOX5 protein in H_V1 immunoprecipitates and H_V1 protein in NOX5 immunoprecipitates from lysates of K562/NOX5 cells, but not control K562 cells (Fig. 5*C*). These results suggest the existence of a specific interaction between H_V1 and NOX5 proteins.

Proton currents were consistently recorded in both K562 (4 of 5 patched cells) and K562/NOX5 cells (12 of 14 cells) voltage-clamped in a perforated-patch configuration (Fig. 5*D*) (35). The current density (*i.e.* current/membrane area) at 40, 50, 60, and 70 mV was larger in K562 cells than in K562/NOX5 cells by a factor of 1.30 on average, although these differences were not statistically significant. The proton channels responded to PMA stimulation with a characteristic array of changes in their behavioral properties, designated enhanced gating mode (negative shift of the g_H-V relationship, faster activation, slower deactivation, increased $g_{H,max}$) (35–37). Most features of the PMA response of proton channels were reversed by the addition of the PKC inhibitor GFX (Fig. 5*D*) (34, 38). These data demonstrate that both K562 cells and K562/NOX5 cells expressed functional proton channels with the characteristic features of H_V1. Collectively, our data in K562 and K562/NOX5 cells demonstrate that a functional interaction exists between H_V1 and NOX5, wherein H_V1 is required for sustaining NOX5-dependent superoxide production.

Similar to the K562/NOX5 cell studies, we found, in human spermatozoa that superoxide production induced by H_2O_2, PMA, or ionomycin was Zn^{2+}-sensitive (Fig. 6*A*) and that H_V1 co-immunopreciptated with NOX5, when the immunoprecipitation was performed with either H_V1 or NOX5 antibodies (Fig. 6*B*). Interestingly, the activated form of c-Abl (p-c-Abl$^{Tyr\text{-}245}$) implicated in NOX5 regulation was also detected in H_V1 immunoprecipitates (Fig. 6*B*), suggesting the existence of a trimolecular complex comprising H_V1, NOX5, and activated c-Abl. Taken together, these results provide strong evidence for

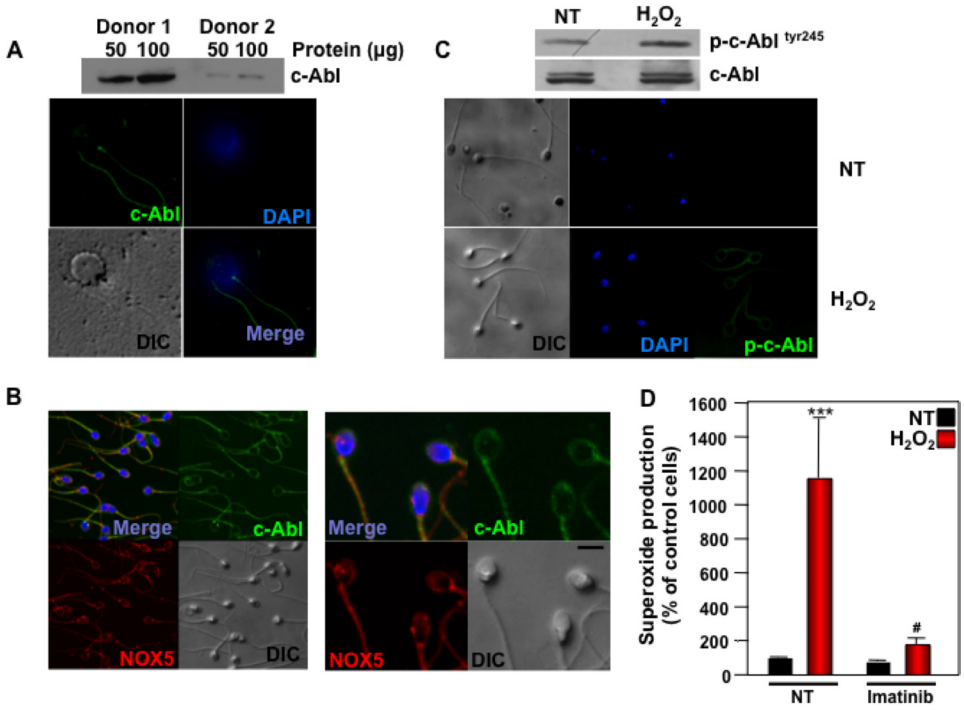

FIGURE 4. **Role of c-Abl in the activation of NOX5 by H_2O_2.** *A, top* is an immunoblot analysis using a c-Abl antibody on human spermatozoa from two different donors. *Bottom* is immunostaining of human spermatozoa with c-Abl antibody and FITC-conjugated secondary antibody (*top left* and *bottom right*), nuclear staining with DAPI (*top right* and *bottom right*), and the DIC image (*bottom left*). *B*, immunostaining of human spermatozoa with c-Abl antibody as in *panel A* (*top left* and *top right*) and NOX5 antibody and Cy™ 3-conjugated secondary antibody (*top left* and *bottom left*), and the differential interference contrast (*DIC*) image (*bottom right*). Note co-localization in the *top left panels*. The *scale bar* indicates a size of 5 μm. *C*, immunoblot analysis (*above*) and immunostaining (*below*, *right panels*) using phospho-c-Abl antibody were performed on human spermatozoa incubated for 10 min with or without (*NT*) 100 μM H_2O_2. DIC images (*left panels*) and DAPI nuclear staining (*middle panels*) are also shown. *D*, superoxide production was determined in sperm cells preincubated for 1 h with 50 μM imatinib and then stimulated for 10 min with 100 μM H_2O_2. Superoxide production was determined as described in the legend to Fig. 2 and expressed as a percent of non-treated cells (*NT*). The data expressed are the mean ± S.E. of 4 independent experiments. *Asterisks* indicate statistical significance *versus* control cells without H_2O_2. ***, $p < 0.001$. *Number sign* indicates statistical significance *versus* cells stimulated with H_2O_2. #, $p < 0.05$.

a functional interaction between H_V1 and NOX5 in human spermatozoa.

Effect of H_2O_2 on Sperm Motility—Because low levels of H_2O_2 can induce sperm capacitation (8, 39, 40) and because H_V1 interacts with NOX5, we tested the effect of H_2O_2 on sperm cell motility. For this we incubated sperm cells with or without 100 μM H_2O_2 for 10 min and then collected motile spermatozoa following the swim-up procedure. The incubation of spermatozoa with H_2O_2 resulted in an increase in the number of sperm in the swim-up fraction (Fig. 7*A*), suggesting that H_2O_2 enhanced spermatozoa motility. To investigate whether the effect of H_2O_2 on motility was due to NOX5, we performed the swim-up experiment in the presence of NOX inhibitors. When spermatozoa were preincubated with DPI or GKT136901, the effect of H_2O_2 on motility was abrogated. These results strongly suggest that the induction of spermatozoa motility by H_2O_2 is dependent on NOX5 activity.

We observed that the effect of H_2O_2 on motility was especially prominent in semen samples that had the lowest baseline percentages of motile sperm. In addition, when we measured superoxide production using spermatozoa collected from the upper fraction after the spontaneous (*i.e.* without H_2O_2) swim-up procedure, these hypermotile spermatozoa did not produce superoxide when stimulated by H_2O_2 compared with pre-swim-up cells (Fig. 7*B*). This finding indicated that following the hyperactivation process spermatozoa are no longer responsive to H_2O_2.

Semen pH-dependent Correlation between Superoxide Production and Sperm Motility—Sperm samples ($n = 128$) were assessed according to the World Health Organization (WHO) laboratory manual (41) for the examination and processing of human semen. Abstinence, defined as the number of days since the previous ejaculation, ranged from 1 to 14 days and was significantly associated with sperm concentration ($r = 0.28$, $p = 0.001$), total sperm cell count ($r = 0.27$, $p = 0.002$), number of motile sperm cells ($r = 0.24$, $p = 0.005$), and concentration of immature forms ($r = 0.32$, $p < 0.001$) (data not shown).

It is known that pH increases during capacitation (42–45). Considering the relationship between H_V1, an important regulator of pH in human spermatozoa, and NOX5, we analyzed the sperm characteristics as a function of semen pH (Table 1), which was categorized into three levels (<8, 8–8.5, and >8.5) for these analyses. Significant differences were found between pH levels for semen viscosity ($p = 0.02$), total sperm count ($p = 0.04$), total number of motile sperm ($p = 0.02$), percent of motile sperm ($p = 0.009$), and sperm progressive motility (progression), which is defined as spermatozoa moving actively, either linearly or in a large circle ($p = 0.04$). Progression was described according to the WHO manual (41) using an ordered categorical scale from 1 to 4, where a higher number indicates a higher progressive motility. Superoxide production did not vary significantly with semen pH. We did observe that a significant difference in basal superoxide production was associated with higher levels of sperm progression (≤2, 3, and >3) ($p =$

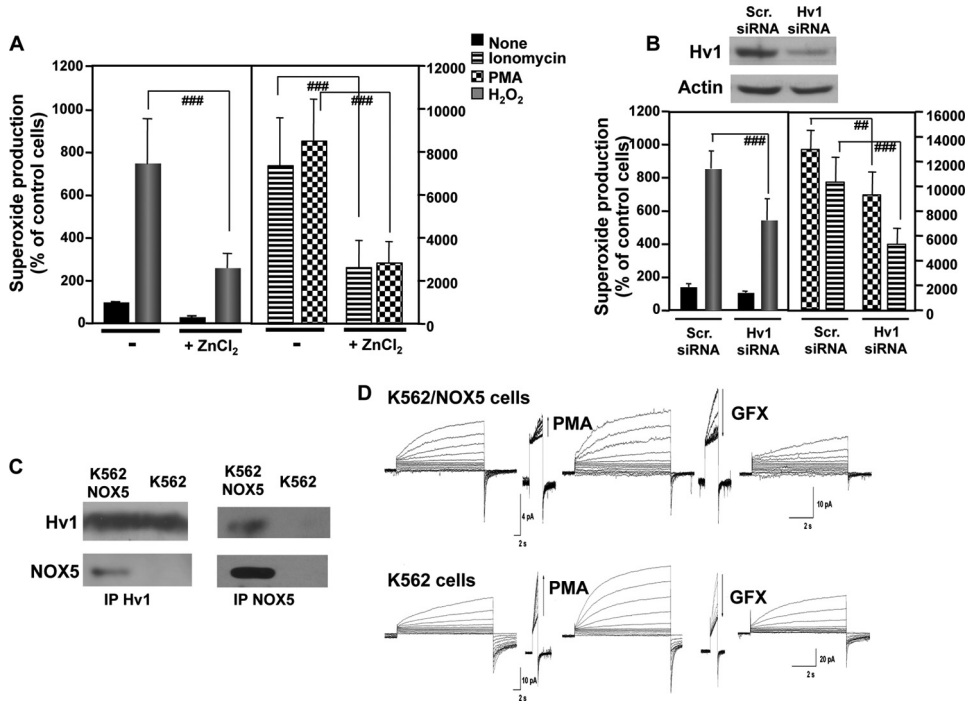

FIGURE 5. **Superoxide production by NOX5 requires H_V1.** *A*, superoxide production by K562/NOX5 cells preincubated for 5 min with or without 1 mM $ZnCl_2$ and then stimulated with ionomycin (1 μM), PMA (1 μg/ml), or H_2O_2 (100 μM) was measured and expressed as described in the legend to Fig. 2. The data expressed are the mean ± S.E. of 6 independent experiments. *Number signs* indicate statistical significance *versus* stimulated cells in the absence of $ZnCl_2$. ###, $p < 0.001$. *B*, K562/NOX5 cells were transiently transfected with scrambled (*scr*) siRNA or H_V1-specific siRNA and tested for superoxide production stimulated by H_2O_2 (100 μM), ionomycin (1 μM), or PMA (1 μg/ml). Immunoblot analysis using H_V1 antibody (*above*) was performed to ensure that the down-regulation of H_V1 protein by siRNA was effective. Actin antibody was used to control for protein loading. The data expressed are the mean ± S.E. of 5 independent experiments. The *number signs* indicate statistical significance *versus* stimulated cells transfected with scrambled siRNA. ##, $p < 0.01$; ###, $p < 0.001$. *C*, immunoprecipitation of NOX5 or H_V1 protein was performed using total protein lysates isolated from K562 cells or K562/NOX5 cells. The content of the immunoprecipitates was analyzed by immunoblot using H_V1 and NOX5 antibodies. The results are representative of 3–5 experiments. *D*, families of proton currents were recorded during pulses in 10-mV increments up to +60 mV in K562 (*lower tracings*) and K562/NOX5 cells (*upper tracings*) before and then after stimulation with PMA (60 nM), and finally after addition of GFX (3 μM).

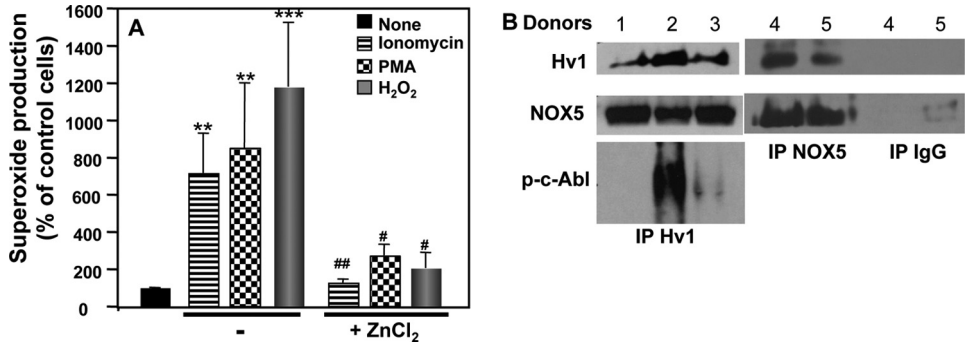

FIGURE 6. **Hv1 activity affects NOX5-dependent superoxide production in human spermatozoa.** *A*, superoxide production by spermatozoa preincubated for 5 min with or without 1 mM $ZnCl_2$ and then stimulated with ionomycin (1 μM), PMA (1 μg/ml), or H_2O_2 (100 μM) was measured and expressed as described in the legend to Fig. 2. The data expressed are the mean ± S.E. of 4–6 independent experiments. *Asterisks* indicate statistical significance *versus* control cells without stimulus. **, $p < 0.01$; ***, $p < 0.001$. The *number signs* indicate statistical significance *versus* stimulated cells in the absence of $ZnCl_2$. ##, $p < 0.01$; ###, $p < 0.001$. *B*, immunoprecipitation of NOX5 or H_V1 protein was performed using total protein lysates isolated from sperm cells of different donors. Non-immune IgG was used to control for specificity. The content of the immunoprecipitates (*IP*) was analyzed by immunoblot using H_V1, NOX5, and phospho-c-Abl antibodies.

0.02). However, superoxide production stimulated by H_2O_2 or PMA were not significantly associated with progression (data not shown).

A regression model was built to analyze for possible correlations among semen pH, sperm motility, and superoxide production, adjusting for abstinence and pH. There appears to be a nonlinear association (inverted U function) between pH and a number of sperm metrics, so we re-categorized pH into levels more conductive to sperm activity (8.0–8.5) and those less conductive to sperm activity (<8 or >8.5) for our regression analyses. The regression model (Table 2) confirmed the previous observations (Table 1), because significant increases in sperm progressive motility (OR = 3.38, 95% CI: 1.25 to 9.15, $p = 0.02$) and percent of motile sperm (mean difference = 14, 95% CI: 4 to 23, $p = 0.004$) were observed for the pH 8.0–8.5 group, compared with the group with either high or low pH values that are less conductive to sperm activity (Table 2). Basal and stimulated (H_2O_2 or PMA) levels of superoxide production tended

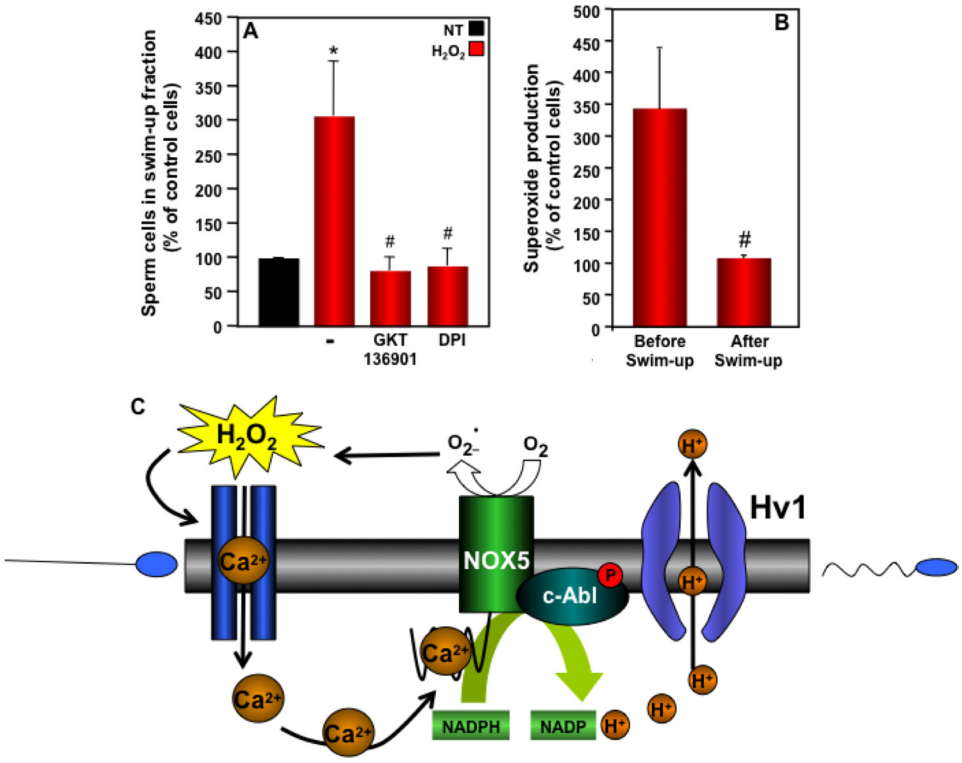

FIGURE 7. **Effect of H_2O_2 on sperm motility.** *A*, from each donor, 2×10^7 spermatozoa preincubated or not with GKT136901 (0.5 μM) or DPI (10 μM) were incubated without (*NT*) or with 100 μM H_2O_2 for 10 min and then subjected to the swim-up procedure. The number of spermatozoa present in the *upper fraction* was determined and expressed as a percent of NT samples. The data expressed are the mean ± S.E. of 10 independent experiments. *Asterisks* indicate statistical significance *versus* control cells without H_2O_2. *, $p < 0.05$. *Number signs* indicate statistical significance *versus* H_2O_2-stimulated cells. #, $p < 0.05$. *B*, the effect of H_2O_2 on superoxide production by spermatozoa before the swim-up procedure and by spermatozoa collected from the upper fraction after the swim-up procedure was determined as described in the legend to Fig. 3. The data represent the percent increase in H_2O_2-induced superoxide formation and are the mean ± S.E. of 4 independent experiments. The *number sign* indicates significance *versus* sperm cells tested before the swim up procedure. #, $p < 0.05$. *C*, hypothetical scheme for the interaction of NOX5 with the H_V1 channel implicated in human spermatozoa hypermotility.

TABLE 1

Semen analysis parameters and superoxide production as a function of semen pH (<8, 8–8.5, and >8.5)

	pH <8 (n=5) Mean ± SD [median]	pH: 8-8.5 (n=107) Mean ± SD [median]	pH >8.5 (n=16) Mean ± SD [median]	P-value[1]
Basal superoxide production (AUC)[3]	911 ± 1040 [559]	11100 ± 49100 [485]	2240 ± 6700 [227]	0.09
H_2O_2 stimulated superoxide production (AUC)[4]	5030 ± 8870 [1230]	30100 ± 80300 [1770]	6160 ± 10600 [911]	0.55
PMA-stimulated superoxide production (AUC)[5]	9790 ± 15900 [2487]	176000 ± 526000 [4603]	54300 ± 145000 [2240]	0.67
Concentration (x10^{-6}/ml)	78.9 ± 65.2 [89.0]	93.1 ± 81.1 [76.2]	45.1 ± 44.9 [21.9]	0.05
Total sperm count (x10^{-6})	292 ± 312 [230]	249 ± 241 [182]	127 ± 189 [38.7]	0.04
Percent of motile sperm	48 ± 28 [60]	52 ± 19 [60]	36 ± 20 [40]	0.009
Total number of motile sperm (x10^{-6})	169 ± 184 [138]	138 ± 140 [99.7]	65.2 ± 120 [19.3]	0.02
Morphology (% Normal)[6]	29 ± 17 [37]	30 ± 18 [30]	25 ± 19 [25]	0.51
Immature forms (x10^{-6}/ml)	2.40 ± 3.91 [0]	2.91 ± 5.67 [0]	1.19 ± 2.42 [0]	0.64
				P-value[2]
Progression, n (%)				0.04
⩽ 2	4 [80]	37 [35]	10 [62]	
3	0 [0]	48 [45]	5 [31]	
>3	1 [20]	22 [21]	1 [6]	
Viscosity[7], n (%)				0.02
0	5 [100]	88 [84]	9 [56]	
> 0	0 [0]	17 [16]	7 [44]	
Agglutination[8], n (%)				0.33
0	3 [60]	53 [50]	5 [31]	
> 0	2 [40]	53 [50]	11 [69]	

[1] Kruskal-Wallis test.
[2] Fisher's exact test.
[3] Missing 25 for pH 8–8.5, 4 for pH >8.5.
[4] Missing 30 for pH 8–8.5, 4 for pH > 8.5.
[5] Missing 38 for pH 8–8.5, 4 for pH >8.5.
[6] Missing 1 for pH 8–8.5.
[7] Missing 2 for pH 8–8.5.
[8] Missing 1 for pH 8–8.5.

TABLE 2

Odds ratio or mean difference of sperm motility and superoxide production for pH 8–8.5 *versus* pH <8 and >8.5

Outcome	pH 8-8.5 vs. pH <8 and >8.5 Odd ratio (95% CI)	P-value[1]
Progression[2]	3.38 (1.25, 9.15)	0.02
	Mean Difference (95% CI)	P-value[3]
Log Total number of sperm	0.85 (0, 1.7)	0.05
Percent of motile sperm	14 (4, 23)	0.004
Log Total number of motile sperm	0.91 (0.09, 1.72)	0.03
Log Basal superoxide production	0.97 (-0.22, 2.16)	0.11
Log H_2O_2 stimulated superoxide production	0.64 (-0.55, 1.84)	0.29
Log PMA-stimulated superoxide production	1.00 (-0.48, 2.47)	0.18

[1] Ordinal logistic regression.
[2] Progression is a 3-level categorical variable (⩽2,3, and >3).
[3] Linear regression of each sperm characteristic in terms of pH with an adjustment for log abstinence.

to be higher in the pH 8.0–8.5 group relative to the pH < 8 or >8.5 group, although these associations were not significant ($p = 0.11$, 0.29, and 0.18 for superoxide production measured under basal condition or stimulated by H_2O_2 or PMA, respectively). Because of the small number of sperm samples in the low plus high pH group, the analysis of sperm motility and superoxide production was conducted only for the median pH group (8.0–8.5) (Table 3). There was a significant correlation between the percent of motile sperm and basal levels of super-

TABLE 3
Association between superoxide production and progression or percent of motile sperm for pH 8–8.5
Analysis was performed among those with pH levels 8–8.5 ($n = 107$).

Predictor	Progression		Percent of motile sperm	
	Odds ratio (95% CI)	p value[a]	Mean difference (95% CI)	p value[b]
Log basal superoxide production ($n = 82$)	1.19 (0.98–1.45)	0.08	1.57 (0.05–3.08)	0.04
Log H_2O_2-stimulated superoxide production ($n = 77$)	1.22 (1–1.5)	0.05	0.35 (−1.02–1.72)	0.61
Log PMA-stimulated superoxide production ($n = 69$)	1.21 (1.01–1.45)	0.04	0.89 (−0.43–2.21)	0.19

[a] Ordinal logistic regression of progression in terms of each measure of superoxide production with an adjustment for log abstinence.
[b] Linear regression of percent of motile sperm in terms of each measure of superoxide production with an adjustment for log abstinence.

oxide production. Although increased superoxide production stimulated by PMA or H_2O_2 was significantly associated with higher progression (H_2O_2-stimulated superoxide production: OR = 1.22, 95% CI: 1.0 to 1.5, $p = 0.05$; PMA-stimulated superoxide production: OR = 1.21, 95% CI: 1.01 to 1.45, $p = 0.04$). These analyses demonstrate that semen pH and sperm superoxide production are closely associated with sperm motility and suggest that the correlation between superoxide production and sperm motility is pH-dependent (Fig. 7*C*).

DISCUSSION

Both physiologic and pathologic effects of ROS in spermatozoa have been described, but the identity of the ROS-producing enzyme(s) has remained unknown. Here, we report for the first time that NOX5 is expressed and functional in human spermatozoa and that its activity is implicated in spermatozoa motility.

Spermatozoa released from the testis are transcriptionally inert (46) and yet they undergo functional maturation to acquire ovum-fertilizing ability. These changes are believed to occur through the modulation of biochemical pathways and cellular properties by incoming signals from the sperm microenvironment, including ROS (47). The putative ROS-producing enzyme has been compared with the NADPH oxidase expressed in phagocytic leukocytes (48). Some studies have even suggested that spermatozoa themselves do not possess NADPH oxidase activity (48–50), but rather that ROS generation is attributable to leukocytes that may be present in some sperm preparations (51–53). Our data show that spermatozoa express their own ROS-producing enzyme, namely one or more of the long splice variants of NOX5 NADPH oxidase, which produce superoxide in a Ca^{2+}-dependent manner. Because a quantitative PCR approach is precluded by the fact that spermatozoa are transcriptionally inert, we tested human sperm samples for other NOX isoforms by immunoblot analyses using antibodies specific for NOX1, -2, and -4. For all donors tested, we were unable to detect any signals. Although we cannot categorically exclude the possibility that other NOX isoforms are expressed, these findings demonstrate that NOX5 is the predominant NOX family NADPH oxidase in human spermatozoa. Further studies are needed to identify the specific *NOX5* splice variants expressed in human spermatozoa.

We reported previously (24) that H_2O_2 positively regulates NOX5β via a Ca^{2+}/c-Abl-dependent pathway. The current studies demonstrate that this regulation is also operative in human spermatozoa, as we observed that both the Ca^{2+} chelator BAPTA and the c-Abl tyrosine kinase inhibitor imatinib mesylate abrogated H_2O_2-induced superoxide production. Furthermore, we provide the first evidence that a functional complex between NOX5 and c-Abl exist in human spermatozoa. ROS-induced tyrosine phosphorylation of several unidentified proteins appears to be essential for sperm capacitation (54). Reminiscent of our findings on the regulation of NOX5 by H_2O_2 (24), two major spermatozoal proteins with molecular sizes similar to NOX5L and c-Abl have been reported to be regulated by PKA and H_2O_2 in a protein-tyrosine phosphatase-independent manner (6, 54, 55). This observation further supports the functional importance of NOX5 and c-Abl in spermatozoa.

A recent report showed that the H_V1 proton channel is likely to be responsible for cytoplasmic alkalinization in human spermatozoa, and that enhanced proton currents correlate with sperm capacitation and hypermotility (29). The physiologic function of these channels has been characterized best in phagocytic leukocytes, where H_V1-dependent H^+ efflux compensates for the membrane depolarization and intracellular acidification generated by the electrogenic NADPH oxidase enzymatic activity (30–33). However, the complex relationship between H_V1 and NADPH oxidase remains incompletely understood. On one hand, robust proton currents in response to PMA are seen only in cells with a high level of NOX2 activity, such as neutrophils (35), eosinophils (56), and PLB-985 cells (57), whereas cells that do not have a high level of NOX2 activity exhibit a weaker response that differs in having a smaller shift of the g_H-V relationship and little or no slowing of deactivation (channel closing) (34, 58). On the other hand, some cell types lack any recordable proton current at all, irrespective of whether they express NADPH oxidase, for example, COS-7 cells (34). To date there is still no systematic correlation between the H_V1 proton current and the expression of a functional NOX. These observations may reflect the complexity of cellular systems that regulate membrane depolarization and pH homeostasis, suggesting that multiple proton generating systems can be coupled to H_V1 and that multiple proton transporters may be linked to NOX enzymes (59, 60). It is also possible that the experimental conditions required to measure proton channel currents are not optimal for detecting weak amplitude proton currents that may result from the activity of NOX isoforms other than NOX2.

We found that the proton current in the response to PMA stimulation in K562 cells was similar in amplitude, channel opening and closing kinetics, and the position of the g_H-V relationship, whether or not NOX5 was heterologously expressed. Because PMA can activate NOX5 and proton channels independently (28, 61), it is difficult to determine whether there is a NOX5-dependent proton current. Unfortunately, in these cells

proton currents stimulated by ionomycin were too small to permit further analysis. The evidence of a functional interaction between H_V1 and NOX5 came rather from analyzing the effect of the H_V1 functional status on NOX5-dependent superoxide production. In particular, we found that H_V1 inhibition by Zn^{2+} or down-regulation by H_V1-specific siRNA reduced NOX5 superoxide-generating activity. This result suggests that, as observed for NOX2, NOX5 superoxide generation requires H_V1 proton channel activity to compensate for depolarization and intracellular acidification to sustain ROS generation. The similar inhibitory effect of Zn^{2+} on NOX5 activity and the co-immunoprecipitation of NOX5 and H_V1 in human spermatozoa strongly suggest that a similar functional interaction exists between NOX5 and H_V1 in these cells.

The Zn^{2+}-rich environment in the semen (62, 63) would tend to prevent premature proton flux through sperm H_V1 channels. Also in line with previous studies on human neutrophils, it is plausible that NOX5 activity precedes H_V1 channel opening. However, because both the intracellular spermatozoal and extracellular pH in the vaginal tract are acidic, it is not readily apparent how NOX5L sustains superoxide production (64). Although NOX5 and H_V1 clearly interact, it remains uncertain whether NOX5 activation is required for H_V1 channel opening or might occur subsequent to H_V1 activation. Little is known about the mechanism by which NOX5S is activated, although pathways involving acidic pH and PKA were shown to induce its activity and/or expression in certain cell types (15, 65, 66). Given the importance of Ca^{2+} signaling in sperm function and the cross-regulation of Ca^{2+} entry by PKA and pH (67, 68), NOX5S, if expressed, could contribute to ROS-mediated sperm function in the acidic environment of the female genital tract (69–71).

The intriguing relationship between H_V1 and NOX5 encouraged us to evaluate the impact of ROS on sperm motility. We found that the induction of superoxide production by H_2O_2 stimulated the motility of sperm cells. However, this effect was observed only in spermatozoa that were not already hyperactivated. The statistical analysis of sperm characteristics *versus* superoxide production confirmed our experimental observation, establishing that pH and superoxide production were both important predictors of spermatozoa motility. Our data showing a functional interaction between the H_V1 proton channel and NOX5 NADPH oxidase, and the trends observed in our statistical analysis, suggest strongly that the correlation between superoxide production and motility is pH-dependent. Interestingly, the novel finding that progesterone, a proposed physiological sperm chemoattractant, is a modulator of the pH-dependent Ca^{2+} channel CatSper (72), provides a potential mechanism for linking Ca^{2+} entry, NOX5 activation, and ROS-stimulated hypermotility, thereby reinforcing the concept of a central role of NOX5 in human sperm motility.

This study provides novel and specific evidence that NOX5 is expressed at the protein level and is functionally active in human spermatozoa. Moreover, the regulation of NOX5 by H_2O_2 is mediated by Ca^{2+} entry and c-Abl tyrosine kinase activation, whereas the downstream ROS generation is implicated in spermatozoa motility. Taken together, our results suggest that the expression levels and/or activities of NOX5, c-Abl, and H_V1 are significant determinants of the redox status of human spermatozoa and consequently their motility and ovum-fertilizing potential. Moreover, NOX5 and the proteins regulating its activity represent new therapeutic targets for either male infertility (if NOX5 is hyperactive) or male contraception (if NOX5 is physiologically active).

Acknowledgments—The confocal microscopy studies were performed in the Institutional Optical Imaging Facility of the University of Texas Health Science Center at San Antonio, which is supported by National Institutes of Health Grants P30 CA054174 (Cancer Therapy and Research Center), P30 AG013319 (Nathan Shock Center), and P01 AG019316 (Aging, Oxidative Stress and Cell Death). We thank Dr. Craig Witz for arranging initial access to human sperm samples from the University of Texas Medicine Fertility Center, Drs. Victoria Frohlich and Shivani Maffi for expert guidance on confocal microscopy image acquisition and analysis, Maria Gamez and Mario de la Pena for expert technical assistance, and Drs. Susan Smith, Yves Gorin, and Denis Feliers for helpful discussions.

REFERENCES

1. MacLeod, J. (1943) The role of oxygen in the metabolism and motility of human spermatozoa. *Am. J. Physiol.* **138,** 512–518
2. Aitken, R. J. (1994) A free radical theory of male infertility. *Reprod. Fertil. Dev.* **6,** 19–23; discussion 23–24
3. Moustafa, M. H., Sharma, R. K., Thornton, J., Mascha, E., Abdel-Hafez, M. A., Thomas, A. J., Jr., and Agarwal, A. (2004) Relationship between ROS production, apoptosis, and DNA denaturation in spermatozoa from patients examined for infertility. *Hum. Reprod.* **19,** 129–138
4. de Lamirande, E., and Gagnon, C. (1992) Reactive oxygen species and human spermatozoa. I. Effects on the motility of intact spermatozoa and on sperm axonemes. *J. Androl.* **13,** 368–378
5. Aitken, R. J. (2000) Possible redox regulation of sperm motility activation. *J. Androl.* **21,** 491–496
6. de Lamirande, E., and Lamothe, G. (2009) Reactive oxygen-induced reactive oxygen formation during human sperm capacitation. *Free Radic. Biol. Med.* **46,** 502–510
7. de Lamirande, E., and Gagnon, C. (1993) Human sperm hyperactivation and capacitation as parts of an oxidative process. *Free Radic. Biol. Med.* **14,** 157–166
8. Aitken, R. J., Ryan, A. L., Baker, M. A., and McLaughlin, E. A. (2004) Redox activity associated with the maturation and capacitation of mammalian spermatozoa. *Free Radic. Biol. Med.* **36,** 994–1010
9. Bánfi, B., Molnár, G., Maturana, A., Steger, K., Hegedûs, B., Demaurex, N., and Krause, K. H. (2001) A Ca^{2+}-activated NADPH oxidase in testis, spleen, and lymph nodes. *J. Biol. Chem.* **276,** 37594–37601
10. Bánfi, B., Tirone, F., Durussel, I., Knisz, J., Moskwa, P., Molnár, G. Z., Krause, K. H., and Cox, J. A. (2004) Mechanism of Ca^{2+} activation of the NADPH oxidase 5 (NOX5). *J. Biol. Chem.* **279,** 18583–18591
11. Fulton, D. J. (2009) Nox5 and the regulation of cellular function. *Antioxid. Redox. Signal* **11,** 2443–2452
12. Cheng, G., Cao, Z., Xu, X., van Meir, E. G., and Lambeth, J. D. (2001) Homologs of $gp91^{phox}$. Cloning and tissue expression of Nox3, Nox4, and Nox5. *Gene* **269,** 131–140
13. Brar, S. S., Corbin, Z., Kennedy, T. P., Hemendinger, R., Thornton, L., Bommarius, B., Arnold, R. S., Whorton, A. R., Sturrock, A. B., Hueckstead, T. P., Quinn, M. T., Krenitsky, K., Ardie, K. G., Lambeth, J. D., and Hoidal, J. R. (2003) NOX5 NAD(P)H oxidase regulates growth and apoptosis in DU 145 prostate cancer cells. *Am. J. Physiol. Cell Physiol.* **285,** C353–369
14. Kamiguti, A. S., Serrander, L., Lin, K., Harris, R. J., Cawley, J. C., Allsup, D. J., Slupsky, J. R., Krause, K. H., and Zuzel, M. (2005) Expression and activity of NOX5 in the circulating malignant B cells of hairy cell leukemia. *J. Immunol.* **175,** 8424–8430

15. BelAiba, R. S., Djordjevic, T., Petry, A., Diemer, K., Bonello, S., Banfi, B., Hess, J., Pogrebniak, A., Bickel, C., and Görlach, A. (2007) NOX5 variants are functionally active in endothelial cells. *Free Radic. Biol. Med.* **42,** 446–459
16. Jay, D. B., Papaharalambus, C. A., Seidel-Rogol, B., Dikalova, A. E., Lassègue, B., and Griendling, K. K. (2008) Nox5 mediates PDGF-induced proliferation in human aortic smooth muscle cells. *Free Radic. Biol. Med.* **45,** 329–335
17. Salles, N., Szanto, I., Herrmann, F., Armenian, B., Stumm, M., Stauffer, E., Michel, J. P., and Krause, K. H. (2005) Expression of mRNA for ROS-generating NADPH oxidases in the aging stomach. *Exp. Gerontol.* **40,** 353–357
18. Cucoranu, I., Clempus, R., Dikalova, A., Phelan, P. J., Ariyan, S., Dikalov, S., and Sorescu, D. (2005) NAD(P)H oxidase 4 mediates transforming growth factor-β1-induced differentiation of cardiac fibroblasts into myofibroblasts. *Circ. Res.* **97,** 900–907
19. Hong, J., Behar, J., Wands, J., Resnick, M., Wang, L. J., Delellis, R. A., Lambeth, D., and Cao, W. (2010) Bile acid reflux contributes to development of esophageal adenocarcinoma via activation of phosphatidylinositol-specific phospholipase Cγ2 and NADPH oxidase NOX5-S. *Cancer Res.* **70,** 1247–1255
20. de Lamirande, E., Tsai, C., Harakat, A., and Gagnon, C. (1998) Involvement of reactive oxygen species in human sperm arcosome reaction induced by A23187, lysophosphatidylcholine, and biological fluid ultrafiltrates. *J. Androl.* **19,** 585–594
21. Sabeur, K., and Ball, B. A. (2007) Characterization of NADPH oxidase 5 in equine testis and spermatozoa. *Reproduction* **134,** 263–270
22. Vijayakumar, R., Ndubisi, B., Prien, S., De Leon, F., and Heine, W. (1986) Quantitative ultramorphological evaluation of swim-up spermatozoa used in human *in vitro* fertilization and transcervical intrauterine insemination. *Arch. Androl.* **17,** 223–230
23. Parrish, J. J., and Foote, R. H. (1987) Quantification of bovine sperm separation by a swim-up method. Relationship to sperm motility, integrity of acrosomes, sperm migration in polyacrylamide gel and fertility. *J. Androl.* **8,** 259–266
24. El Jamali, A., Valente A. J., Lechleiter, J. D., Gamez, M. J., Pearson, D. W., Nauseef, W. M., and Clark, R. A. (2008) Novel redox-dependent regulation of NOX5 by the tyrosine kinase c-Abl. *Free Radic. Biol. Med.* **44,** 868–881
25. Petheo, G. L., Orient, A., Baráth, M., Kovács, I., Réthi, B., Lányi, A., Rajki, A., Rajnavölgyi, E., and Geiszt, M. (2010) Molecular and functional characterization of Hv1 proton channel in human granulocytes. *PloS One* **5,** e14081
26. Laleu, B., Gaggini, F., Orchard, M., Fioraso-Cartier, L., Cagnon, L., Houngninou-Molango, S., Gradia, A., Duboux, G., Merlot, C., Heitz, F., Szyndralewiez, C., and Page, P. (2010) First in class, potent, and orally bioavailable NADPH oxidase isoform 4 (Nox4) inhibitors for the treatment of idiopathic pulmonary fibrosis. *J. Med. Chem.* **53,** 7715–7730
27. Sedeek, M., Callera, G., Montezano, A., Gutsol, A., Heitz, F., Szyndralewiez, C., Page, P., Kennedy, C. R., Burns, K. D., Touyz, R. M., and Hébert, R. L. (2010) Critical role of Nox4-based NADPH oxidase in glucose-induced oxidative stress in the kidney. Implications in type 2 diabetic nephropathy. *Am. J. Physiol. Renal Physiol.* **299,** F1348-F1358
28. Jagnandan, D., Church, J. E., Banfi, B., Stuehr, D. J., Marrero, M. B., and Fulton, D. J. (2007) Novel mechanism of activation of NADPH oxidase 5. Calcium sensitization via phosphorylation. *J. Biol. Chem.* **282,** 6494–6507
29. Lishko, P. V., Botchkina, I. L., Fedorenko, A., and Kirichok, Y. (2010) Acid extrusion from human spermatozoa is mediated by flagellar voltage-gated proton channel. *Cell* **140,** 327–337
30. Morgan, D., Capasso, M., Musset, B., Cherny, V. V., Ríos, E., Dyer, M. J., and DeCoursey, T. E. (2009) Voltage-gated proton channels maintain pH in human neutrophils during phagocytosis. *Proc. Natl. Acad. Sci. U.S.A.* **106,** 18022–18027
31. Ramsey, I. S., Ruchti, E., Kaczmarek, J. S., and Clapham, D. E. (2009) Hv1 proton channels are required for high-level NADPH oxidase-dependent superoxide production during the phagocyte respiratory burst. *Proc. Natl. Acad. Sci. U.S.A.* **106,** 7642–7647
32. DeCoursey, T. E. (2010) Voltage-gated proton channels find their dream job managing the respiratory burst in phagocytes. *Physiology* **25,** 27–40
33. El Chemaly, A., Okochi, Y., Sasaki, M., Arnaudeau, S., Okamura, Y., and Demaurex, N. (2010) VSOP/Hv1 proton channels sustain calcium entry, neutrophil migration, and superoxide production by limiting cell depolarization and acidification. *J. Exp. Med.* **207,** 129–139
34. Morgan, D., Cherny, V. V., Price, M. O., Dinauer, M. C., and DeCoursey, T. E. (2002) Absence of proton channels in COS-7 cells expressing functional NADPH oxidase components. *J. Gen. Physiol.* **119,** 2477–2486
35. DeCoursey, T. E., Cherny, V. V., Zhou, W., and Thomas, L. L. (2000) Simultaneous activation of NADPH oxidase-related proton and electron currents in human neutrophils. *Proc. Natl. Acad. Sci. U.S.A.* **97,** 6885–6889
36. Bánfi, B., Schrenzel, J., Nüsse, O., Lew, D. P., Ligeti, E., Krause, K. H., and Demaurex, N. (1999) A novel H^+ conductance in eosinophils. Unique characteristics and absence in chronic granulomatous disease. *J. Exp. Med.* **190,** 183–194
37. Bánfi, B., Maturana, A., Jaconi, S., Arnaudeau, S., Laforge, T., Sinha, B., Ligeti, E., Demaurex, N., and Krause, K. H. (2000) A mammalian H^+ channel generated through alternative splicing of the NADPH oxidase homolog NOH-1. *Science* **287,** 138–142
38. Morgan, D., Cherny, V. V., Finnegan, A., Bollinger, J., Gelb, M. H., and DeCoursey, T. E. (2007) Sustained activation of proton channels and NADPH oxidase in human eosinophils and murine granulocytes requires PKC but not cPLA2α activity. *J. Physiol.* **579,** 327–344
39. Aitken, R. J., and Vernet, P. (1998) Maturation of redox regulatory mechanisms in the epididymis. *J. Reprod. Fertil. Suppl.* **53,** 109–118
40. de Lamirande, E., and O'Flaherty, C. (2008) Sperm activation. Role of reactive oxygen species and kinases. *Biochim. Biophys. Acta* **1784,** 106–115
41. World Health Organization, and Department of Reproductive Health and Research (2010) Examination and processing of human semen. 5th Ed., WHO, Geneva, Switzerland
42. Neri-Vidaurri Pdel, C., Torres-Flores, V., and González-Martínez, M. T. (2006) A remarkable increase in the pH_i sensitivity of voltage-dependent calcium channels occurs in human sperm incubated in capacitating conditions. *Biochem. Biophys. Res. Commun.* **343,** 105–109
43. Garcia, M. A., and Meizel, S. (1999) Regulation of intracellular pH in capacitated human spermatozoa by a Na^+/H^+ exchanger. *Mol. Reprod. Dev.* **52,** 189–195
44. Zeng, Y., Oberdorf, J. A., and Florman, H. M. (1996) pH regulation in mouse sperm. Identification of Na^+-, Cl^--, and HCO_3^--dependent and arylaminobenzoate-dependent regulatory mechanisms and characterization of their roles in sperm capacitation. *Dev. Biol.* **173,** 510–520
45. Florman, H. M., Jungnickel, M. K., and Sutton, K. A. (2010) Shedding light on sperm fertility. *Cell* **140,** 310–312
46. Sotolongo, B., and Ward, W. S. (2000) DNA loop domain organization. The three-dimensional genomic code. *J. Cell Biochem. Suppl.* **35,** 23–26
47. Aitken, R. J., Baker, M. A., De Iuliis, G. N., and Nixon B. (2010) New insights into sperm physiology and pathology. *Handb. Exp. Pharmacol.* **198,** 99–115
48. Armstrong, J. S., Bivalacqua, T. J., Chamulitrat, W., Sikka, S., and Hellstrom, W. J. (2002) A comparison of the NADPH oxidase in human sperm and white blood cells. *Int. J. Androl.* **25,** 223–229
49. Ford, W. C., Whittington, K., and Williams, A. C. (1997) Reactive oxygen species in human sperm suspensions. Production by leukocytes and the generation of NADPH to protect sperm against their effects. *Int. J. Androl.* **20,** 44–49
50. Richer, S. C., and Ford, W. C. (2001) A critical investigation of NADPH oxidase activity in human spermatozoa. *Mol. Hum. Reprod.* **7,** 237–244
51. Aitken, R. J., and West, K. M. (1990) Analysis of the relationship between reactive oxygen species production and leukocyte infiltration in fractions of human semen separated on Percoll gradients. *Int. J. Androl.* **13,** 433–451
52. Kessopoulou, E., Tomlinson, M. J., Barratt, C. L., Bolton, A. E., and Cooke, I. D. (1992) Origin of reactive oxygen species in human semen. Spermatozoa or leucocytes? *J. Reprod. Fertil.* **94,** 463–470
53. Whittington, K., and Ford, W. C. (1999) Relative contribution of leukocytes and of spermatozoa to reactive oxygen species production in human

sperm suspensions. *Int. J. Androl.* **22,** 229–235
54. Aitken, R. J., Harkiss, D., Knox, W., Paterson, M., and Irvine, D. S. (1998) A novel signal transduction cascade in capacitating human spermatozoa characterized by a redox-regulated, cAMP-mediated induction of tyrosine phosphorylation. *J. Cell Sci.* **111,** 645–656
55. Rivlin, J., Mendel, J., Rubinstein, S., Etkovitz, N., and Breitbart, H. (2004) Role of hydrogen peroxide in sperm capacitation and acrosome reaction. *Biol. Reprod.* **70,** 518–522
56. DeCoursey, T. E., Cherny, V. V., DeCoursey, A. G., Xu, W., and Thomas, L. L. (2001) Interactions between NADPH oxidase-related proton and electron currents in human eosinophils. *J. Physiol.* **535,** 767–781
57. DeCoursey, T. E., Cherny, V. V., Morgan, D., Katz, B. Z., and Dinauer, M. C. (2001) The gp91^{phox} component of NADPH oxidase is not the voltage-gated proton channel in phagocytes, but it helps. *J. Biol. Chem.* **276,** 36063–36066
58. Capasso, M., Bhamrah, M. K., Henley, T., Boyd, R. S., Langlais, C., Cain, K., Dinsdale, D., Pulford, K., Khan, M., Musset, B., Cherny, V. V., Morgan, D., Gascoyne, R. D., Vigorito, E., DeCoursey, T. E., MacLennan, I. C., and Dyer, M. (2010) HVCN1 modulates BCR signal strength via regulation of BCR-dependent generation of reactive oxygen species. *Nat. Immunol.* **11,** 265–272
59. Resch, C. T., Winogrodzki, J. L., Häse, C. C., and Dibrov, P. (2011) Insights into the biochemistry of the ubiquitous NhaP family of cation/H^+ antiporters. *Biochem. Cell Biol.* **89,** 130–137
60. Morth, J. P., Pedersen, B. P., Buch-Pedersen, M. J., Andersen, J. P., Vilsen, B., Palmgren, M. G., and Nissen, P. (2011) A structural overview of the plasma membrane Na^+,K^+-ATPase and H^+-ATPase ion pumps. *Nat. Rev. Mol. Cell Biol.* **12,** 60–70
61. Musset, B., Capasso, M., Cherny, V. V., Morgan, D., Bhamrah, M., Dyer, M. J., and DeCoursey, T. E. (2010) Identification of Thr^{29} as a critical phosphorylation site that activates the human proton channel Hvcn1 in leukocytes. *J. Biol. Chem.* **285,** 5117–5121
62. Rogers, C., Bernstein, G., Nakamura, R., Endahl, G., Bhoopat, T. (1988) Vaginal fluid zinc concentration as a marker for intercourse. *J. Forensic Sci.* **33,** 77–83
63. Alexandrino, A. P., Rodrigues M. A., Matsuo, T., Gregório, E. P., Santilli, J. C. (2011) Evaluation of seminal zinc levels by atomic absorption in men with spinal cord injury. *Spinal Cord* **49,** 435–438
64. Morgan, D., Cherny, V. V., Murphy, R., Katz, B. Z., and DeCoursey, T. E. (2005) The pH dependence of NADPH oxidase in human eosinophils. *J. Physiol.* **569,** 419–431
65. Fu, X., Beer, D. G., Behar, J., Wands, J., Lambeth, D., and Cao, W. (2006) cAMP-response element-binding protein mediates acid-induced NADPH oxidase NOX5-S expression in Barrett esophageal adenocarcinoma cells. *J. Biol. Chem.* **281,** 20368–20382
66. Si, J., Fu, X., Behar, J., Wands, J., Beer, D. G., Souza, R. F., Spechler, S. J., Lambeth, D., and Cao, W. (2007) NADPH oxidase NOX5-S mediates acid-induced cyclooxygenase-2 expression via activation of NF-κB in Barrett esophageal adenocarcinoma cells. *J. Biol. Chem.* **282,** 16244–16255
67. Teves, M. E., Guidobaldi, H. A., Uñates, D. R., Sanchez, R., Miska, W., Publicover, S. J., Morales Garcia, A. A., and Giojalas, L. C. (2009) Molecular mechanism for human sperm chemotaxis mediated by progesterone. *PloS One* **4,** e8211
68. Lishko, P. V., and Kirichok, Y. (2010) The role of Hv1 and CatSper channels in sperm activation. *J. Physiol.* **588,** 4667–4672
69. White, D. R., and Aitken, R. J. (1989) Relationship between calcium, cyclic AMP, ATP, and intracellular pH and the capacity of hamster spermatozoa to express hyperactivated motility. *Gamete Res.* **22,** 163–177
70. de Lamirande, E., Jiang, H., Zini, A., Kodama, H., and Gagnon, C. (1997) Reactive oxygen species and sperm physiology. *Rev. Reprod.* **2,** 48–54
71. De Jonge, C. (2005) Biological basis for human capacitation. *Hum. Reprod. Update* **11,** 205–214
72. Lishko, P. V., Botchkina, I. L., and Kirichok, Y. (2011) Progesterone activates the principal Ca^{2+} channel of human sperm. *Nature* **471,** 387–391